The formation of waves in a gas-liquid two-layer channel flow

Iain Bethune[1], Lennon Ó Náraigh*[2], David Scott[1], Peter Spelt[3,4], Prashant Valluri[5], Zlatko Solomenko[3]

[1]Edinburgh Parallel Computing Centre, University of Edinburgh, James Clerk Maxwell Building, Mayfield Road, Edinburgh EH9 3JZ, UK
[2]School of Mathematics and Statistics, University College Dublin, Ireland
[3]Département Mécanique, Université de Lyon 1
[4]Laboratoire de Mécanique des Fluides et dAcoustique (LMFA), CNRS, Ecole Centrale de Lyon, 69134 Ecully, France
[5]School of Engineering, University of Edinburgh, Kings Buildings, Edinburgh EH9 3JL, UK

4th December 2018

This project has received funding from the European Union's Horizon 2020 Research and Innovation Programme under grant agreement No 778104

THERMASMART
Thermal Management of Microprocessors

Context

Two-phase stratified flow is ubiquitous in nature and industry.

(a) Kelvin-Helmholtz instability

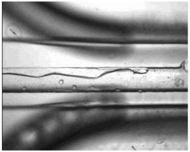

(b) Stratified flow in pipelines

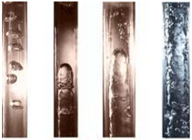

(c) Slug flow

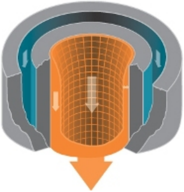

(d) Falling-film reactors

- Mathematically, and computationally, a tough problem – turbulence, extreme nonlinearity, topological change in interfaces, a range of instabilities that need to be captured.
- Even the laminar regime is tough - current focus of the research.

Structure of talk

This talk has three parts:

1. Technical overview of in-house TPLS solver
2. TPLS – a scientific case study involving hydrodynamic instability
3. Outlook, future work, and new collaborations

Context: The numerical challenge

- Flows involving many length- and time-scales
- Flows with sharp changes in interfacial topologies
- Transient three-dimensional simulations required over long periods of time, requiring **scalable** codes run at very high **resolutions**.

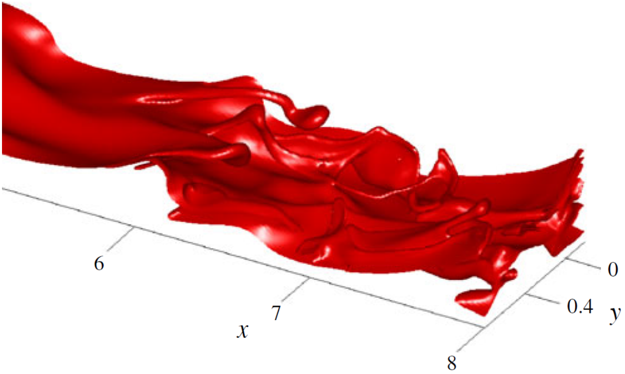

Context: Existing methodologies

- Existing interface-capturing methods: Levelset, Volume of Fluid, Particles, Diffuse Interface Method

Context: Existing methodologies

- Existing interface-capturing methods: Levelset, Volume of Fluid, Particles, Diffuse Interface Method
- Existing implementations: Open-source (e.g. Gerris, etc.), Commercial (CFX, etc.), in-house solvers.

Context: Existing methodologies

- Existing interface-capturing methods: Levelset, Volume of Fluid, Particles, Diffuse Interface Method
- Existing implementations: Open-source (e.g. Gerris, etc.), Commercial (CFX, etc.), in-house solvers.
- Some drawbacks (not respectively): Black-box approach, validation uncertain, artificial diffusion. Key drawbacks: resolution constraints, scalability.

Context: Existing methodologies

- Existing interface-capturing methods: Levelset, Volume of Fluid, Particles, Diffuse Interface Method
- Existing implementations: Open-source (e.g. Gerris, etc.), Commercial (CFX, etc.), in-house solvers.
- Some drawbacks (not respectively): Black-box approach, validation uncertain, artificial diffusion. Key drawbacks: resolution constraints, scalability.
- Our in-house code **TPLS** addresses these issues, in particular **resolution and scalability**.

Context: Existing methodologies

- Existing interface-capturing methods: Levelset, Volume of Fluid, Particles, Diffuse Interface Method
- Existing implementations: Open-source (e.g. Gerris, etc.), Commercial (CFX, etc.), in-house solvers.
- Some drawbacks (not respectively): Black-box approach, validation uncertain, artificial diffusion. Key drawbacks: resolution constraints, scalability.
- Our in-house code **TPLS** addresses these issues, in particular **resolution and scalability**.
- Not a silver bullet – levelset methods – tradeoff between capturing interfacial topology with great fidelity, and mass loss. But mass loss minimized at high resolution.

TPLS: Equations of motion

Numerical solution of two-phase Navier–Stokes equations with interface capturing:

$$\rho(\phi)\left(\frac{\partial \boldsymbol{u}}{\partial t}+\boldsymbol{u}\cdot\nabla\boldsymbol{u}\right)=-\nabla p+\frac{1}{\mathrm{Re}}\nabla\cdot\left[\mu(\phi)\left(\nabla\boldsymbol{u}+\nabla\boldsymbol{u}^{T}\right)\right]+\boldsymbol{f}_{\mathrm{st}}(\phi)-\rho(\phi)\mathcal{G}\hat{\boldsymbol{z}},$$

where $\nabla\cdot\mathbf{u}=0$ and ϕ is the interface-capturing field:

TPLS: Equations of motion

Numerical solution of two-phase Navier–Stokes equations with interface capturing:

$$\rho(\phi)\left(\frac{\partial \boldsymbol{u}}{\partial t}+\boldsymbol{u}\cdot\nabla\boldsymbol{u}\right)=-\nabla p+\frac{1}{\mathrm{Re}}\nabla\cdot\left[\mu(\phi)\left(\nabla\boldsymbol{u}+\nabla\boldsymbol{u}^{T}\right)\right]+\boldsymbol{f}_{\mathrm{st}}(\phi)-\rho(\phi)\mathcal{G}\hat{\boldsymbol{z}},$$

where $\nabla\cdot\mathbf{u}=0$ and ϕ is the interface-capturing field:

Levelset method:

$$\frac{\partial\phi}{\partial t}+\boldsymbol{u}\cdot\nabla\phi=0,\qquad \boldsymbol{f}_{\mathrm{st}}=\delta_{\epsilon}(\phi)\frac{1}{\mathrm{We}}\widehat{\boldsymbol{n}}\nabla\cdot\widehat{\boldsymbol{n}}.\qquad \widehat{\boldsymbol{n}}=\frac{\nabla\phi}{|\nabla\phi|}.$$

TPLS: Equations of motion

Numerical solution of two-phase Navier–Stokes equations with interface capturing:

$$\rho(\phi)\left(\frac{\partial \boldsymbol{u}}{\partial t}+\boldsymbol{u}\cdot\nabla\boldsymbol{u}\right)=-\nabla p+\frac{1}{\mathrm{Re}}\nabla\cdot\left[\mu(\phi)\left(\nabla\boldsymbol{u}+\nabla\boldsymbol{u}^{T}\right)\right]+\boldsymbol{f}_{\mathrm{st}}(\phi)-\rho(\phi)\mathcal{G}\hat{\boldsymbol{z}},$$

where $\nabla\cdot\mathbf{u}=0$ and ϕ is the interface-capturing field:

Levelset method:

$$\frac{\partial\phi}{\partial t}+\boldsymbol{u}\cdot\nabla\phi=0,\qquad \boldsymbol{f}_{\mathrm{st}}=\delta_{\epsilon}(\phi)\frac{1}{\mathrm{We}}\widehat{\boldsymbol{n}}\nabla\cdot\widehat{\boldsymbol{n}}.\qquad \widehat{\boldsymbol{n}}=\frac{\nabla\phi}{|\nabla\phi|}.$$

Dimensionless groups:

$$\mathrm{Re}=\frac{\rho_T V L}{\mu_T},\qquad \mathcal{G}=\frac{gL}{V^2},\qquad \mathrm{We}=\frac{\rho_T L V^2}{\gamma},$$

(I also use $\mathcal{S}=1/\mathrm{We}$, for historical reasons!)

TPLS: Problem geometry and configuration

- Simple channel geometry: periodic boundary conditions at $x = 0$, $x = L_x$; walls (no slip) at $z = 0$, $z = L_z$.
- Constant pressure drop drives flow in streamwise direction (forcing).
- Basic version involves hydrodynamics only. TPLS with physics under development, for applications including contact-line dynamics, and mass transfer.

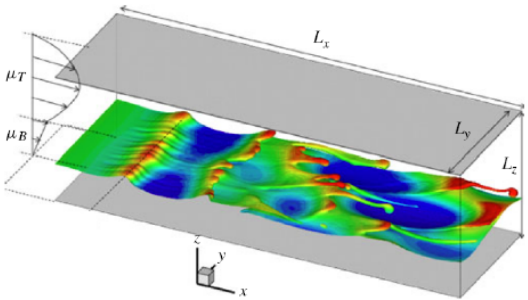

TPLS: Numerical discretization schemes

- Marker-and-cell discretization: pressures, densities, viscosities, and ϕ at cell centres, velocities at cell faces.

TPLS: Numerical discretization schemes

- Marker-and-cell discretization: pressures, densities, viscosities, and ϕ at cell centres, velocities at cell faces.
- Finite-volumes, with flux-conservative differencing for the momentum equation.

TPLS: Numerical discretization schemes

- Marker-and-cell discretization: pressures, densities, viscosities, and ϕ at cell centres, velocities at cell faces.
- Finite-volumes, with flux-conservative differencing for the momentum equation.
- Momentum step: centred differences for the convective derivative, Crank–Nicholson treatment for the diffusion, third-order Adams–Bashforth for the time evolution.

TPLS: Numerical discretization schemes

- Marker-and-cell discretization: pressures, densities, viscosities, and ϕ at cell centres, velocities at cell faces.
- Finite-volumes, with flux-conservative differencing for the momentum equation.
- Momentum step: centred differences for the convective derivative, Crank–Nicholson treatment for the diffusion, third-order Adams–Bashforth for the time evolution.
- Projection method: Momenta are updated first, followed by a correction step involving a pressure update, thereby enforcing incompressibility.

TPLS: Numerical discretization schemes

- Marker-and-cell discretization: pressures, densities, viscosities, and ϕ at cell centres, velocities at cell faces.
- Finite-volumes, with flux-conservative differencing for the momentum equation.
- Momentum step: centred differences for the convective derivative, Crank–Nicholson treatment for the diffusion, third-order Adams–Bashforth for the time evolution.
- Projection method: Momenta are updated first, followed by a correction step involving a pressure update, thereby enforcing incompressibility.
- The levelset function $\phi(x, y, z, t)$ is carried with the flow (3rd-order WENO) but is corrected at each timestep ('redistancing').

TPLS: Parallel computing

- Typical runs involve up to 10 million gridpoints, meaning that large-scale parallel simulation is unavoidable (larger runs (up to 100 million gridpoints) are also performed).

TPLS: Parallel computing

- Typical runs involve up to 10 million gridpoints, meaning that large-scale parallel simulation is unavoidable (larger runs (up to 100 million gridpoints) are also performed).
- Code is parallelized using MPI; parallelization scheme takes account of problem geometry (2D domain decomposition)

TPLS: Parallel computing

- Typical runs involve up to 10 million gridpoints, meaning that large-scale parallel simulation is unavoidable (larger runs (up to 100 million gridpoints) are also performed).
- Code is parallelized using MPI; parallelization scheme takes account of problem geometry (2D domain decomposition)
- Data is outputted to files periodically using parallel I/O – NetCDF data storage.
- The portable version of the code uses simple hand-coded algorithms for linear algebra steps (e.g. presusre step). A version on the UK supercomputer Archer exists where these have been replaced these by a Krylov solver using repeated calls to the PETSc library.

TPLS: Parallel computing

- Typical runs involve up to 10 million gridpoints, meaning that large-scale parallel simulation is unavoidable (larger runs (up to 100 million gridpoints) are also performed).
- Code is parallelized using MPI; parallelization scheme takes account of problem geometry (2D domain decomposition)
- Data is outputted to files periodically using parallel I/O – NetCDF data storage.
- The portable version of the code uses simple hand-coded algorithms for linear algebra steps (e.g. presusre step). A version on the UK supercomputer Archer exists where these have been replaced these by a Krylov solver using repeated calls to the PETSc library.

TPLS: Parallel computing

- Typical runs involve up to 10 million gridpoints, meaning that large-scale parallel simulation is unavoidable (larger runs (up to 100 million gridpoints) are also performed).
- Code is parallelized using MPI; parallelization scheme takes account of problem geometry (2D domain decomposition)
- Data is outputted to files periodically using parallel I/O – NetCDF data storage.
- The portable version of the code uses simple hand-coded algorithms for linear algebra steps (e.g. presusre step). A version on the UK supercomputer Archer exists where these have been replaced these by a Krylov solver using repeated calls to the PETSc library.
- Parallel efficiency with 2000 MPI processes is only 0.6 – there is a tradeoff between robustness/simplicity and performance. Underscores the rationale behind replacing the hand-coded linear-algebra solvers with libraries.

Strict benchmarks for code's accuracy

- Introduce a tiny sinusoidal perturbation at the interface.
- Produces pressure and velocity fluctuations that satisfy linear equations of motion.
- Linearized equations of motion solved via eigenvalue analysis (independent, quasi-analytical).
- Gives growth rate and wave speed of wave-like fluctuations.

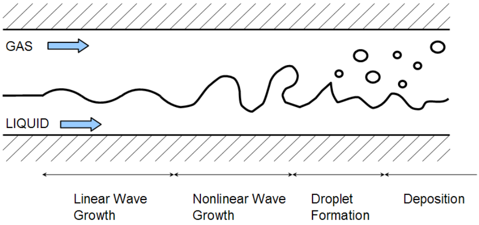

Focus on finding agreement between OS analysis and wave growth in the code.

Orr–Sommerfeld analysis – Results

Stratified co-flow test case (h=0.3)

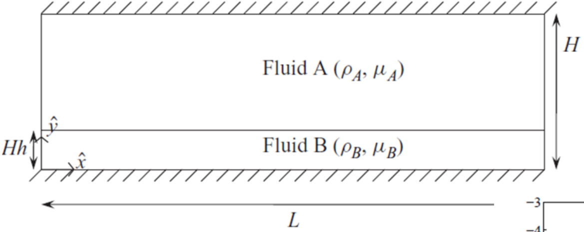

$$(Re, r, m, \mathcal{S}) = (100, 1, 30, 0.01)$$

- *L x W x H = (3 x 1 x 1)*
- *12 million grid points*
- *1024 processors, 12 h*

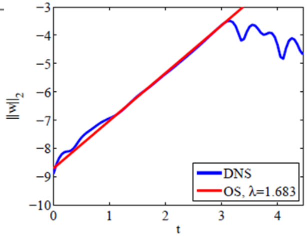

Application of TPLS: where do 3D waves in parallel flows come from?

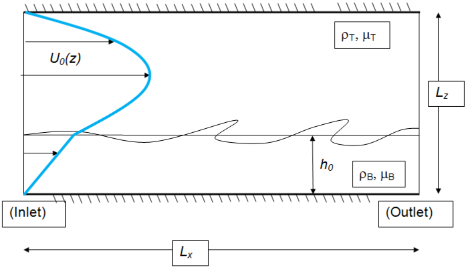

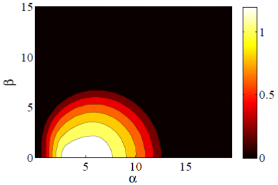

$$r = 1, \mathcal{S} = 0.1$$

Linear instability of 2D parallel flow is dominated by 2D waves.
So how do 3D structures form?

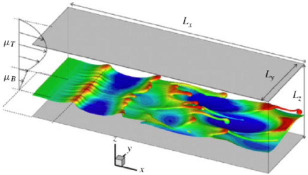

Brief review for liquid-liquid flows

We know the answer for liquid-liquid flows ($r = 1$) – it is weakly nonlinear analysis.

Streamwise waves – Large temporal growth, Spanwise waves – No temporal growth rate

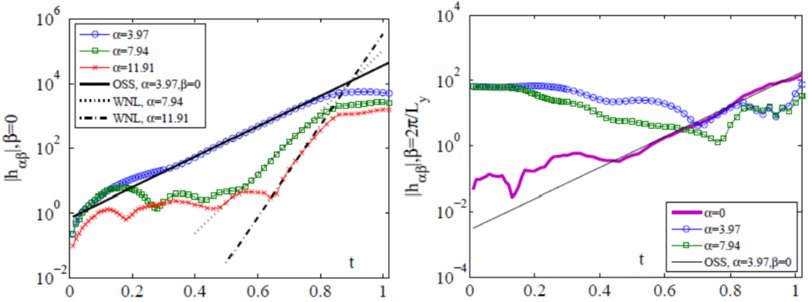

- Streamwise overtones are enslaved to the streamwise dominant mode
- Purely spanwise mode enslaved to the dominant streamwise mode

Periodic boundary conditions, $(Re, m, r, \mathcal{S}) = (300, 30, 1, 0.3)$.

New study required for gas-liquid flows

For gas-liquid flows, linear theory predicts a **direct route**.

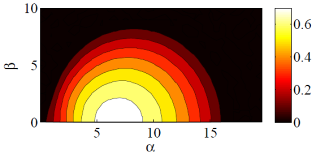

(a) $r = 100, \mathcal{S} = 0.1$

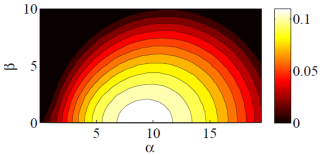

(b) $r = 1000, \mathcal{S} = 0.1$

Eigenvalue analysis of the two-phase Orr–Sommerfeld–Squire equations for $Re = 100$, $m = 30$, $h_0 = 0.3$, and $\mathcal{S} = 0.1$, and $\mathcal{G} = 0.1$.

New study required for gas-liquid flows

For gas-liquid flows, linear theory predicts a **direct route**.

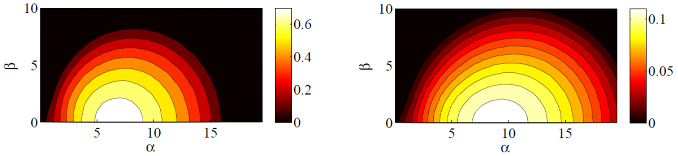

(a) $r = 100, \mathcal{S} = 0.1$ (b) $r = 1000, \mathcal{S} = 0.1$

Eigenvalue analysis of the two-phase Orr–Sommerfeld–Squire equations for $Re = 100$, $m = 30$, $h_0 = 0.3$, and $\mathcal{S} = 0.1$, and $\mathcal{G} = 0.1$.

Overall trend: increasing r means that more modes become unstable (both streamwise and spanwise), but with a smaller growth rate.

Theoretical Prediction confirmed by DNS

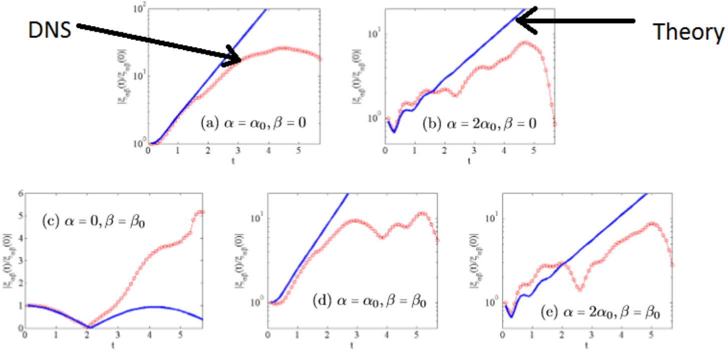

DNS results (lines with circles) for the case ($m = 50, h_0 = 0.2, \mathcal{G} = 0.1, \mathrm{We} = 10$), with $r = 1000$ and $\mathrm{Re} = 500$. Shown also is a comparison with linearized DNS (unadorned lines). Here, $\alpha_0 = 2\pi/L_x$ and $\beta_0 = 2\pi/L_y$ denote the fundamental wavenumber in the streamwise and spanwise directions respectively. In panel (c) the growth of the relevant amplitude is modest and a vertical linear (as opposed to logarithmic) scale is used. Also, the 'kink' at $t = 2$ in the same panel simply corresponds to a a zero of $\xi_{0\beta_0}(t)$, as this particular Fourier amplitude does not grow exponentially.

2D-DNS used to construct a flow-pattern map

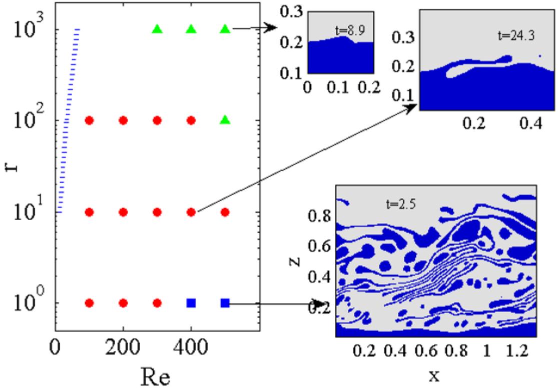

Flow-pattern map for the two-dimensional simulations. The non-dimensionalization is based on the upper-layer properties, with $(m = 50, h_0 = 0.2, \mathcal{G} = 0.1, \mathrm{We} = 10)$. Squares – Dispersed liquid phase. Circles – ligaments. Triangle – saturated travelling wave. The insets show snapshots of the three different flow regimes.

Carefully-chosen 3D simulations show the results carry over

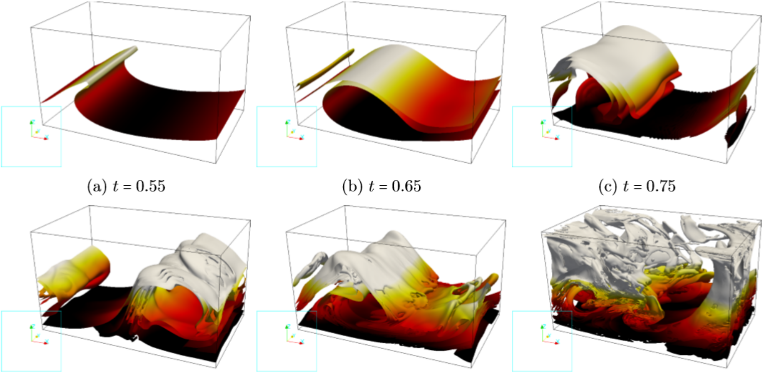

(a) $t = 0.55$ (b) $t = 0.65$ (c) $t = 0.75$

(d) $t = 0.8$ (e) $t = 0.85$ (f) $t = 0.95$

DNS results for the case $(m = 50, h_0 = 0.2, \mathcal{G} = 0.1, \mathrm{We} = 10)$, with $r = 1$ and $\mathrm{Re} = 500$.

The case $r = 10$

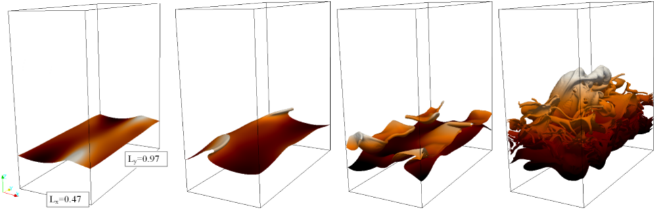

(a) $t = 0.4$ (b) $t = 0.5$ (c) $t = 0.6$ (d) $t = 0.7$

FIG. 30. DNS results for the case $(m = 50, h_0 = 0.2, \mathcal{G} = 0.1, \mathrm{We} = 10)$, with $r = 10$ and $\mathrm{Re} = 500$.

The case $r = 100$

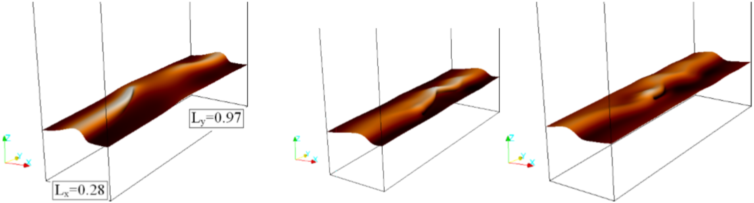

(a) $t = 1.1$ (b) $t = 1.4$ (c) $t = 1.6$

DNS results for the case $(m = 50, h_0 = 0.2, \mathcal{G} = 0.1, \mathrm{We} = 10)$, with $r = 100$ and $\mathrm{Re} = 500$.

Summary of Scientific Findings

- Using TPLS, we answer the question, where do 3D waves in parallel flows come from?

Summary of Scientific Findings

- Using TPLS, we answer the question, where do 3D waves in parallel flows come from?
- For liquid-liquid flows an indirect (weakly nonlinear) mechanism prevails.

Summary of Scientific Findings

- Using TPLS, we answer the question, where do 3D waves in parallel flows come from?
- For liquid-liquid flows an indirect (weakly nonlinear) mechanism prevails.
- Using theory and DNS, our current work shows a different scenario at work in gas-liquid flows:
    - The interfacial waves in gas-liquid flows grow much more slowly than those in corresponding liquid-liquid flows.
    - However, a wider range of wavenumbers (both streamwise and spanwise) are unstable for the gas-liquid case.

Summary of Scientific Findings

- Using TPLS, we answer the question, where do 3D waves in parallel flows come from?
- For liquid-liquid flows an indirect (weakly nonlinear) mechanism prevails.
- Using theory and DNS, our current work shows a different scenario at work in gas-liquid flows:
  - The interfacial waves in gas-liquid flows grow much more slowly than those in corresponding liquid-liquid flows.
  - However, a wider range of wavenumbers (both streamwise and spanwise) are unstable for the gas-liquid case.

Therefore, three-dimensional waves form in gas-liquid flows via a **direct route**: by waiting long enough, streamwise and spanwise modes form as a result of small-amplitude perturbations.

Summary of Scientific Findings

- Using TPLS, we answer the question, where do 3D waves in parallel flows come from?
- For liquid-liquid flows an indirect (weakly nonlinear) mechanism prevails.
- Using theory and DNS, our current work shows a different scenario at work in gas-liquid flows:
    - The interfacial waves in gas-liquid flows grow much more slowly than those in corresponding liquid-liquid flows.
    - However, a wider range of wavenumbers (both streamwise and spanwise) are unstable for the gas-liquid case.

> Therefore, three-dimensional waves form in gas-liquid flows via a **direct route**: by waiting long enough, streamwise and spanwise modes form as a result of small-amplitude perturbations.

- Beyond this early-stage wave growth, a zoo of different phenomena is possible, depending on the particular flow parameters involved.

Outlook, future work, and new collaborations

TPLS is ripe for application and extension. The following work is soon to get under way:

1. New Physics – heat transfer between the phases
2. Understanding experimental results – mircofluidics

New Physics – work is ongoing to add a temperature scalar field to TPLS.

- There will be a separate temperature field in each phase.
- The model will incorporate heat transfer across the interface using the levelset methodology.
- A flow-pattern map will be constructed, and the Nusselt number for different flow configurations (flat interface, waves, ligaments, suspensions) will be calculated.
- This will enable us to characterize the effect of complex flow on heat transfer.

Understanding experimental results

- TPLS in its current configuration involves a uniform grid – this means it can't really handle turbulence (outside of a large-eddy simulation framework).
- Hence, TPLS is restricted to low-to-intermediate $\mathrm{Re} \lesssim 500$.
- This is an **opportunity**, as it tells us where to focus research efforts.
- One particularly promising area is **microfluidics**, where the Reynolds numbers are exactly within the range suitable for TPLS – Chaotic interfacial motion in may be a route to efficient mixing in 'lab on a chip' microfluidics devices.

Microfluidics I

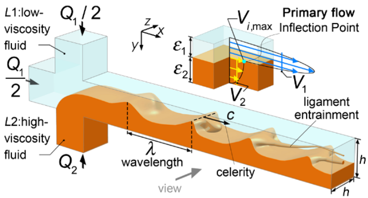

Hu and Cubaoud, PRL 2018

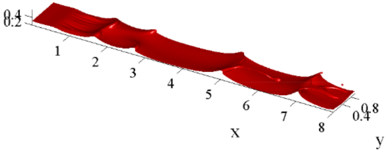

Ó Náraigh and collaborators, JFM, 2014 (TPLS)

Microfluidics II

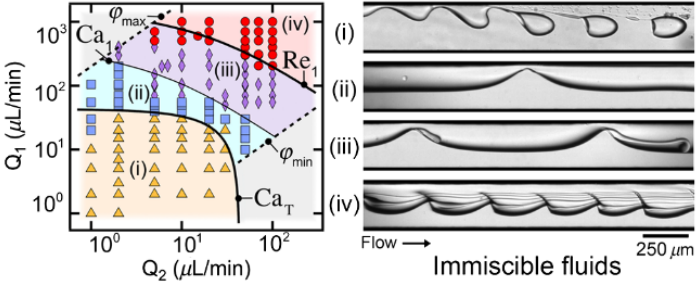

- Experimental flow-pattern map from Hu and Cubaoud (PRL 2018)
- Potential now to generate the same flow-pattern maps using theory (stability analysis) and DNS, thereby optimizing microfluidic two-phase mixing

New Collaborations

- New collaborations always welcome.
- To facilitate potential new collaborations, TPLS is open source!

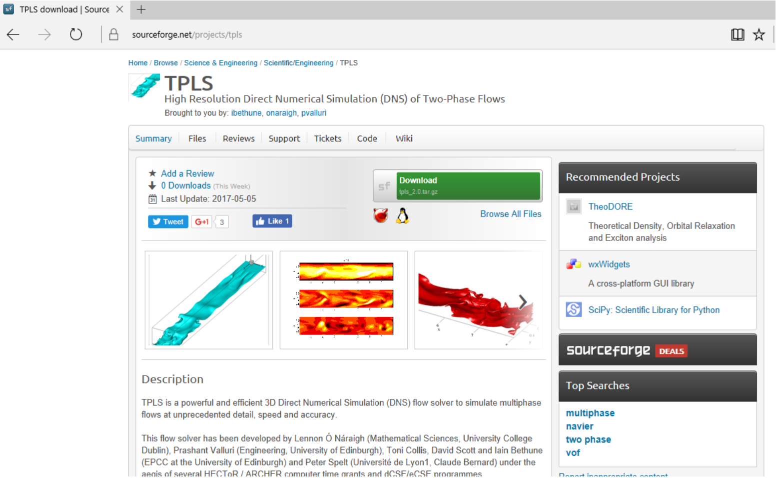

Reminder

- IUTAM symposium in multiphase flows, special applications in heat transfer – June 2019, Dublin
- Followed immediately by Thermasmart midterm review meeting